Dalton Transactions

Accepted Manuscript

ROYAL SOCIETY OF CHEMISTRY

www.rsc.org/dalton

Revised DT-ART-01-2014-000090.R1

Reactions of Trinuclear Platinum Clusters with Electrophiles: An Example of Ionisation Isomerism with $[Pt_3(\mu\text{-}I)(\mu\text{-}PPh_2)_2(PPh_3)_3]I$ and $[Pt_3(\mu\text{-}PPh_2)_2I_2(PPh_3)_3]$. Molecular Structures of $[Pt_3(\mu\text{-}Cl)(\mu\text{-}PPh_2)_2(PPh_3)_3]PF_6$, $[Pt_3(\mu\text{-}PPh_2)_2I_2(PPh_3)_3]\cdot C_6H_5Cl$ and of the Mixed-Metal Pt-Ag Cluster $[Pt_3\{\mu_3\text{-}AgBF_4\}(\mu\text{-}I)(\mu\text{-}PPh_2)_2(PPh_3)_3]BF_4$.†

Christine Archambault,[a] Robert Bender,[a] Pierre Braunstein,*[,a] Yves Dusausoy[b] and Richard Welter.[c]

[a] *Laboratoire de Chimie de Coordination (UMR 7177 CNRS), Institut de Chimie, Université de Strasbourg, 4 rue Blaise Pascal, F-67081 Strasbourg-Cédex, France, Fax: + 33 368851308. E-mail: braunstein@unistra.fr*

[b] *Laboratoire de Cristallographie et Modélisation des Matériaux Minéraux et Biologiques, UPRESA 7036, Université Henri Poincaré, Nancy I, Faculté des Sciences, Boîte postale 239, F-54206 Vandoeuvre-les-Nancy, France.*

[c] *Laboratoire DECOMET, Institut de Chimie (UMR 7177 CNRS), Université de Strasbourg, 4 rue Blaise Pascal, F-67081 Strasbourg-Cedex, France*.

† CCDC 980719 (**4**(PF_6)), 980720 ([Pt_3(μ-Br)(μ-PPh_2)$_2$(PPh_3)$_3$]OH), 978243 (**5**·PhCl) and 678244 (**11**(BF_4)) contain the supplementary crystallographic data for the structures reported. These data can be obtained free of charge via http://www.ccdc.cam.ac.uk/conts/retrieving.html, or from the Cambridge Crystallographic Data Centre, 12 Union Road, Cambridge CB2 1EZ, UK; fax: (+44) 1223-336-033; or e-mail: deposit@ccdc.cam.ac.uk.

Abstract

The reaction of the 44 electron cluster $[Pt_3(\mu\text{-}PPh_2)_3Ph(PPh_3)_2]$ (**1**) with wet $AgBF_4$ afforded the cationic cluster $[Pt_3(\mu\text{-}OH)(\mu\text{-}PPh_2)_2(PPh_3)_3]BF_4$ (**3**(BF_4)). The latter slowly transformed in $[Pt_3(\mu\text{-}Cl)(\mu\text{-}PPh_2)_2(PPh_3)_3]BF_4$ (**4**(BF_4)) upon recrystallization from CH_2Cl_2. These 44 electron clusters have been characterized by $^{31}P\{^1H\}$ NMR and the crystal structure of **4**(PF_6) was determined by X-ray diffraction, as well as that of $[Pt_3(\mu\text{-}PPh_2)_2I_2(PPh_3)_3]$ (**5**), which was obtained by recrystallization of the known cluster $[Pt_3(\mu\text{-}I)(\mu\text{-}PPh_2)_2(PPh_3)_3]I$ (**2**(I)) from toluene and represents a neutral formula isomer of the latter. In addition, we have prepared the adducts of cluster **1** containing the moieties $[Cu(NCMe)_2]^+$ and $[Au(PPh_3)]^+$ in **6** and **7**, respectively, and on the basis of their spectroscopic data, it was concluded that these complexes have similar structures to that previously established for the adduct of **1** with Ag(TFA) (TFA = $OC(O)CF_3$), $[Pt_3\{\mu_3\text{-}Ag(TFA)\}(\mu\text{-}PPh_2)_3Ph(PPh_3)_2]$ (**8**). The cationic clusters in **3**(BF_4) and **4**(BF_4) react with Ag(TFA) to afford cationic adducts in $[Pt_3\{\mu_3\text{-}Ag(TFA)\}(\mu\text{-}X)(\mu\text{-}PPh_2)_2(PPh_3)_3]BF_4$ (**9**, X = OH; **10**, X = Cl). The structure of the mixed-metal cluster $[Pt_3(\mu_3\text{-}AgBF_4)(\mu\text{-}I)(\mu\text{-}PPh_2)_2(PPh_3)_3]BF_4$ (**11**), obtained by reaction of the complex **2**(I) with $AgBF_4$, was determined by X-ray diffraction.

Introduction.

Polynuclear phosphido-bridged platinum complexes represent a class of complexes that continues to attract considerable interest because of the diversity of structures and nuclearities encountered,[1] and their rich and often unexpected reactivity, which can involve both the phosphido ligands and the metals.[2] The bridging phosphido ligand usually derives from the thermal activation of a metal-coordinated tertiary phosphine or the oxidative addition of the P-H bond of a secondary phosphine to a zerovalent metal complex and the stabilizing role of the 3 electron donor phosphido bridge(s) is well documented.[1,3,4] The flexibility of the Pt-(μ-P)-Pt angle, which can be readily monitored by ^{31}P NMR spectroscopy,[1,5] allows retention or loss, without complex decomposition, of metal-metal bonding.[1,4,6]

Our own work on homometallic phosphido-bridged platinum complexes has mostly focused on the synthesis, structure and reactivity of di- and trinuclear systems.[4,7] In the course of studies on the reactivity of the mixed-valence (2 Pt(I) + 1 Pt(II)) 44 electron cluster $[Pt_3(\mu\text{-}PPh_2)_3Ph(PPh_3)_2]$ (**1**),[4,8] which is obtained by thermolysis of $[Pt(C_2H_4)(PPh_3)_2]$ and shows a unique example of core isomerism depending solely on the crystallization solvent,[4] we have observed that a coupling reaction between a PPh_2 bridge and the phenyl group, to give a PPh_3 ligand, can be induced by oxidation with I_2 while the integrity of the cluster is preserved in the product, the 44 electron

cationic cluster $[Pt_3(\mu\text{-}I)(\mu\text{-}PPh_2)_2(PPh_3)_3]I$ (**2**(I)).[9] This reaction represents the reverse of the thermally-induced P-C bond activation of a coordinated PPh_3 ligand which leads to the synthesis of **1**.[4]

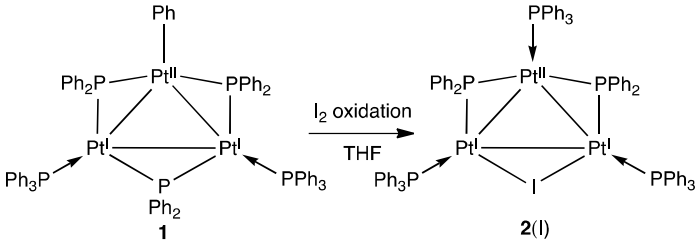

Scheme 1. Oxidation-induced reductive coupling of the phenyl and a μ-PPh_2 group.[9] In all the schemes, a Pt-Pt line is drawn to indicate that the metal-metal distance is consistent with significant bonding interactions between the metals. These lines should not be understood as representing 2c,2e bonding and in the 44 electron clusters, such as **1** and $\mathbf{2}^+$, the three Pt-Pt interactions correspond to 4e,3c bonding.[4]

This reactivity triggered our interest for further studies of the behaviour of **1** toward electrophilic reagents. The electron-rich character of **1** was further demonstrated by its reaction with Ag(TFA) (TFA = trifluoroacetate, $OC(O)CF_3$) which led to the formation of the 1:1 adduct $[Pt_3\{\mu_3\text{-}Ag(TFA)\}(\mu\text{-}PPh_2)_3Ph(PPh_3)_2]$, with retention of the Pt-phenyl bond.[9]

We present here the synthesis and characterization of further relevant triplatinum clusters and of MPt_3 clusters (M = Cu, Ag, Au) in which the electrophilic coinage metal caps the triangular face of the platinum cluster.

Results and Discussion

Reactivity of $[Pt_3(\mu\text{-}PPh_2)_3Ph(PPh_3)_2]$ (1) and Crystal Structure of $[Pt_3(\mu_2\text{-}Cl)(\mu\text{-}PPh_2)_2(PPh_3)_3]PF_6$ (**4**(PF_6)).

The reaction of **1** with wet $AgBF_4$ in THF afforded the cluster $[Pt_3(\mu_2\text{-}OH)(\mu\text{-}PPh_2)_2(PPh_3)_3](BF_4)$ (**3**(BF_4)) (equation 1).

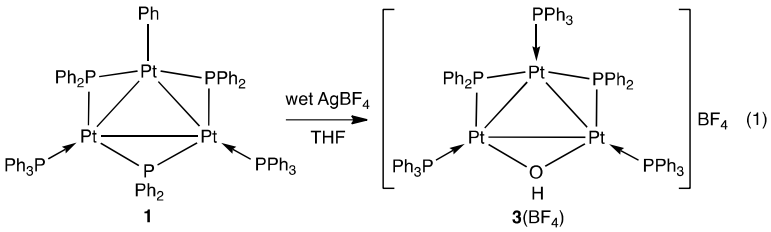

Consistent with this formulation, its FAB-mass spectrum contains peaks at *m/z* = 1759.2 ($[Pt_3(\mu_2\text{-}OH)(\mu\text{-}PPh_2)_2(PPh_3)_3]^+$ = $[M\text{-}BF_4]^+$ and 1742.1 $[M\text{-}BF_4\text{-}OH]^+$. In CH_2Cl_2 solution, **3**(BF_4) slowly transforms in $[Pt_3(\mu_2\text{-}Cl)(\mu\text{-}PPh_2)_2(PPh_3)_3]BF_4$ (**4**(BF_4)) in which a chlorido bridge has replaced the hydroxo bridge of the precursor. This cluster has been characterized by its FAB-mass spectrum and its $^{31}P\{^1H\}$ NMR spectrum. The $^{31}P\{^1H\}$ NMR data of the cationic clusters in **3**(BF_4) and **4**(BF_4) (Table 1, Figure 1) are similar to that of $[Pt_3(\mu\text{-}I)(\mu\text{-}PPh_2)_2(PPh_3)_3]I$ (**2**(I)).[9]

Complex **4**(PF_6) was obtained by reaction of a solution of cluster **1** in THF with one equivalent of HPF_6 in water. Recrystallization of the product from a mixture of CH_2Cl_2 and diethyl ether afforded pale orange crystals suitable for X-ray diffraction (see below).

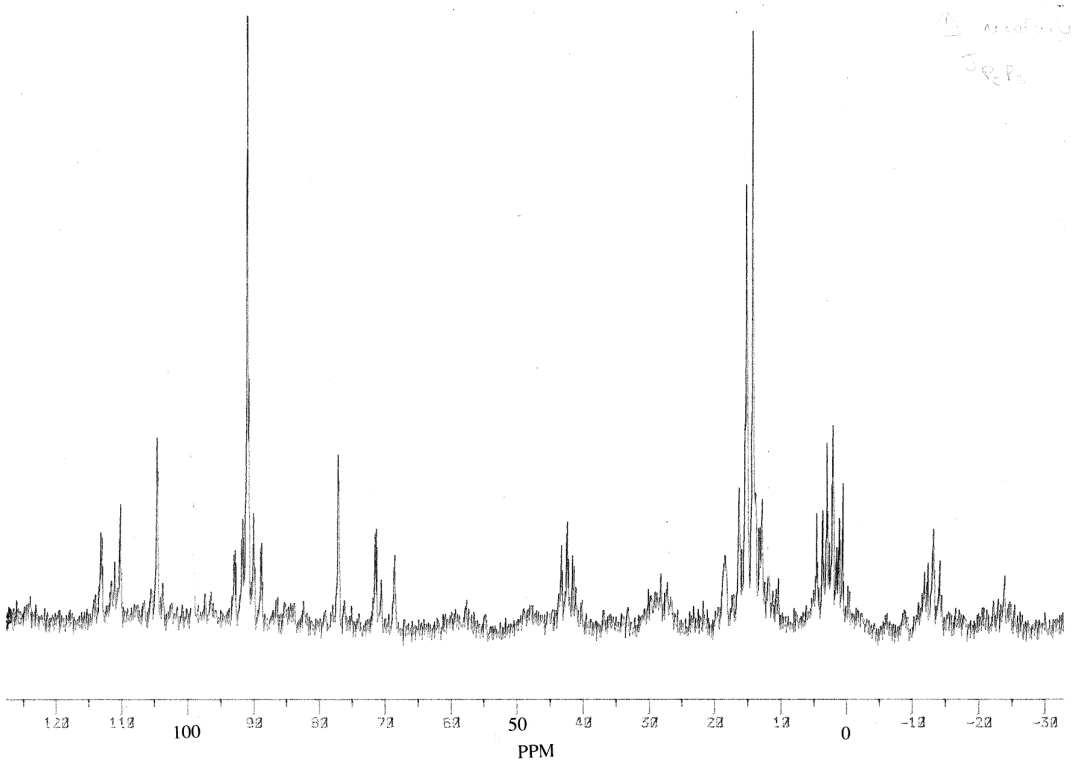

Figure 1. $^{31}P\{^1H\}$ NMR spectrum of $[Pt_3(\mu_2\text{-}OH)(\mu\text{-}PPh_2)_2(PPh_3)_3](BF_4)$ (**3**(BF_4)) in THF.

Table 1. Comparative $^{31}P\{^{1}H\}$ NMR data [δ (ppm), *J* (Hz)] for the cationic clusters $[Pt_3(\mu_2\text{-}X)(\mu\text{-}PPh_2)_2(PPh_3)_3]^+$ in **3**(BF_4), **4**(PF_6), **2**(I)[9] and **2**(BF_4) and the neutral cluster $[Pt_3(\mu\text{-}PPh_2)_2I_2(PPh_3)_3]$ (**5**).[a,b]

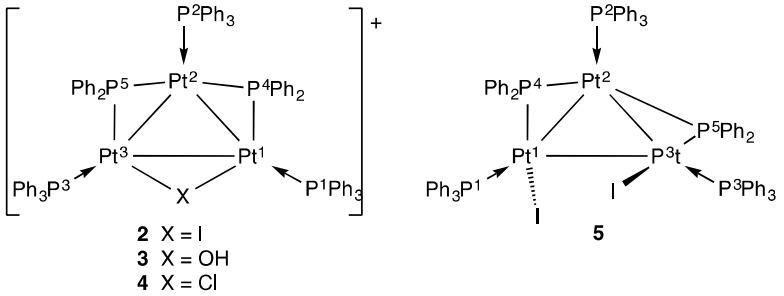

2 X = I
3 X = OH
4 X = Cl

5

	3(BF_4)[c]	**4**(PF_6)[d]	**2**(I)[c]	**2**(BF_4)[d]	**5**[e]
$\delta_{P(1)}$, $\delta_{P(3)}$	14.6	16.7	20.9	19.9	26.7
$\delta_{P(2)}$	2.1	3.4	6.9	6.4	10.0
$\delta_{P(4)}$, $\delta_{P(5)}$	90.8	127.7	155.3	156.4	147.4
$^{1}J_{P(1)\text{-}Pt(1)}$ / $^{1}J_{P(3)\text{-}Pt(3)}$	4495	4405	4312	4296	4498
$^{2}J_{P(1)\text{-}Pt(2)}$ / $^{2}J_{P(3)\text{-}Pt(2)}$	209	192	196	191	243
$^{2}J_{P(2)\text{-}Pt(1)}$ / $^{2}J_{P(2)\text{-}Pt(3)}$	248	231	232	224	268
$^{1}J_{P(2)\text{-}Pt(2)}$	4221	4142	4148	4127	4288
$^{1}J_{P(4)\text{-}Pt(1)}$ / $^{1}J_{P(5)\text{-}Pt(3)}$	3379	3532	3353	3326	3512
$^{1}J_{P(4)\text{-}Pt(2)}$ / $^{1}J_{P(5)\text{-}Pt(2)}$	2229	2264	2299	2290	2366
$^{2}J_{P(4)\text{-}Pt(3)}$ / $^{2}J_{P(5)\text{-}Pt(1)}$	94	96	91	103	47
$^{3}J_{P(1)\text{-}P(2)}$ / $^{3}J_{P(2)\text{-}P(3)}$	76	77	76	74	80
$^{2}J_{P(2)\text{-}P(4)}$ / $^{2}J_{P(2)\text{-}P(5)}$	7				
$^{2}J_{P(4)\text{-}P(5)}$	230	240	235	244	216

[a] The atom numbering corresponds to that shown in Figure 2. [b] The $^{31}P\{^{1}H\}$ NMR spectrum illustrated in ref. 9 which was assigned to **2**(I) in toluene actually corresponds to that of the neutral cluster **5** that has now been fully identified. The $^{31}P\{^{1}H\}$ NMR spectrum of a cationic cluster **3**(BF_4) in THF is now illustrated in Figure 1. [c] In THF. [d] In CH_2Cl_2. [e] In toluene.

The $^{31}P\{^{1}H\}$ NMR spectra of complexes **3**(BF_4) and **4**(PF_6) contain each three sets of signals for the five ^{31}P nuclei, two phosphines and two phosphide bridges being chemically equivalent. Each set is flanked by satellites due to ^{195}Pt–P couplings. The signal at low field is characteristic of two symmetrical phosphorus nuclei bridging two Pt–Pt bonds in a Pt_3 triangle.[4] The other two signals appear as a doublet and a triplet between δ = 2.0 and 26.7 and are attributable to two chemically equivalent phosphines and a unique phosphine which are mutually strongly coupled, respectively.

The doublet signal is characteristic of a P→Pt-Pt←P chain.[10] All these features point to the arrangement of the P and Pt atoms shown above for the cationic clusters **2**-**4**.

When the ionic cluster **2**(I), previously obtained according to Scheme 1,[9] was recrystallized from chlorobenzene, a neutral formula isomer was obtained, $[Pt_3(\mu\text{-}PPh_2)_2I_2(PPh_3)_3]$ (**5**), and this ionisation isomerism was evidenced by the X-ray structure determination of the latter (Figure 3). As expected, the $^{31}P\{^1H]$ NMR data of the cations in **2**(I) and **2**(BF_4) in CH_2Cl_2 are comparable, but there are slight differences between the spectra of **2**(I) and **5** (Table 1).

The $^{31}P\{^1H]$ NMR data of complexes **2**-**5** show that recombination of a bridging PPh_2 group with the phenyl ligand in **1** has occurred to generate a terminal phosphine ligand. This reactivity was first observed when **1** was reacted with I_2 to give **2**(I).[9] The oxidation-induced reductive coupling between a μ-PPh_2 and a phenyl ligand has been confirmed here by the resolution of the crystal structure of **4**(PF_6) by X-ray diffraction.

Molecular Structure of the Cluster $[Pt_3(\mu_2\text{-}Cl)(\mu\text{-}PPh_2)_2(PPh_3)_3]PF_6$ (4(PF_6))

An X-ray diffraction analysis allowed to establish the structure of this complex, which is analogous to **4**(BF_4) (Figure 2, Table 2).

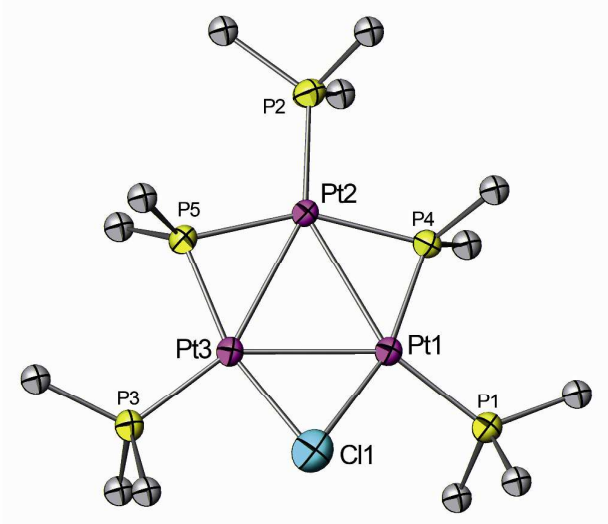

Figure 2. ORTEP view of the cation **4** in $[Pt_3(\mu\text{-}Cl)(\mu\text{-}PPh_2)_2(PPh_3)_3]PF_6$ (**4**(PF_6)) with partial labelling scheme. The ellipsoids enclose 50% of the electronic density. Only the ipso phenyl carbons are shown for clarity.

Table 2. Selected Bond Distances (Å) and Angles (°) in $[Pt_3(\mu\text{-}Cl)(\mu\text{-}PPh_2)_2(PPh_3)_3]PF_6$ (**4**(PF_6))

Pt(1) – Pt(2)	2.904(1)	Cl – Pt(1) – P(1)	90.4(2)
Pt(1) – Pt(3)	2.825(1)	Cl – Pt(1) – P(4)	163.0(2)
Pt(2) – Pt(3)	2.901(1)	P(1) – Pt(1) – P(4)	105.1(2)
Pt(1) – Cl	2.366(8)	Pt(1) – Pt(2) – P(2)	154.5(1)
Pt(1) – P(1)	2.254(5)	Pt(1) – Pt(2) – P(4)	48.1(1)
Pt(1) – P(4)	2.184(6)	Pt(3) – Pt(2) – P(2)	146.9(1)
Pt(2) – P(2)	2.255(6)	Pt(3) – Pt(2) – P(5)	48.3(1)
Pt(2) – P(4)	2.261(5)	P(2) – Pt(2) – P(4)	106.9(2)
Pt(2) – P(5)	2.288(5)	P(2) – Pt(2) – P(5)	98.6(2)
Pt(3) – Cl	2.394(8)	P(4) – Pt(2) – P(5)	154.4(2)
Pt(3) – P(3)	2.230(6)	Pt(1) – Pt(3) – P(3)	142.1(2)
Pt(3) – P(5)	2.193(5)	Pt(1) – Pt(3) – Cl	54.1(2)
Pt(2) – Pt(1) – Pt(3)	60.8(1)	Pt(2) – Pt(3) – P(3)	153.6(2)
Pt(1) – Pt(2) – Pt(3)	58.2(1)	Pt(2) – Pt(3) – P(5)	51.1(1)
Pt(1) – Pt(3) – Pt(2)	60.9(1)	P(3) – Pt(3) – P(5)	103.6(2)
Pt(2) – Pt(1) – P(1)	155.0(2)	Cl – Pt(3) – P(3)	91.4(2)
Pt(2) – Pt(1) – P(4)	50.3(1)	Cl – Pt(3) – P(5)	164.9(2)
Pt(3) – Pt(1) – P(1)	143.6(2)	Pt(1) – Cl – Pt(3)	72.8(2)
Pt(3) – Pt(1) – Cl	54.1(2)	Pt(1) – P(4) – Pt(2)	81.6(2)
		Pt(2) – P(5) – Pt(3)	80.7(2)

The structure of the cation $[Pt_3(\mu_2\text{-}Cl)(\mu\text{-}PPh_2)_2(PPh_3)_3]^+$ (**4**) is based on an almost isosceles Pt_3 triangle, in which the Pt-Pt edges are bridged by two PPh_2 groups and one chlorine atom, each Pt atom being further ligated by a PPh_3 ligand (Figure 2). The Pt(1)-Pt(2) and Pt(2)-Pt(3) bond distances of 2.904(1) and 2.901(1) Å, respectively, and the Pt(1)-Pt(3) distance of 2.825(1) Å are consistent with significant metal-metal interactions (Table 2). The P(2) atom is leaning towards P(5) and makes a P(2)-Pt(2)-P(4) angle of 106.9(2*)*°, while the value of the P(2)-Pt(2)-P(5) angle is 98.6(2)°. In addition, all the donor atoms, i.e. Cl, P(1), P(2), P(3), P(4) and P(5), lie out of the plane of the metallic core by 0.226(9) Å, -0.173(5) Å, -0.138(5) Å, -0.412(6) Å, 0.095(5) Å and -0.168(5) Å, respectively, in an asymmetric manner.

In the course of reactions between **1** (present as an impurity in a batch of a dinuclear Pt(I)-Pt(I) complex whose reactivity was investigated independently[7c]) and HBr in water, we obtained a few crystals of $[Pt_3(\mu\text{-}Br)(\mu\text{-}PPh_2)_2(PPh_3)_3]OH$ after recrystallisation from CH_2Cl_2 and diethyl

ether. These were identified by X-ray diffraction as containing a cationic core very similar to that of $[Pt_3(\mu_2\text{-}Cl)(\mu\text{-}PPh_2)_2(PPh_3)_3]^+$ (**4**) and structural details are provided in the Supplementary Information for comparison.

Molecular Structure of the neutral cluster $[Pt_3(\mu\text{-}PPh_2)_2I_2(PPh_3)_3]$ (5) in 5·PhCl

Single crystals of $[Pt_3(\mu\text{-}PPh_2)_2I_2(PPh_3)_3]$·PhCl (**5**·PhCl) were analysed by X-ray diffraction. The three Pt atoms in **5** form an isosceles triangle different from that in **4** (Pt(1)-Pt(2) = 2.8330(6) Å, Pt(1)-Pt(3) = 2.8334(6) Å and Pt(2)-Pt(3) = 2.8835(7) Å) (Table 3 and Figures 3 and S1). Two Pt-Pt edges are bridged by a PPh_2 group and each Pt atom bears a PPh_3 ligand. This neutral cluster also possesses two terminal iodo ligands linked to Pt(1) and Pt(3), respectively, which are situated on opposite sides of the metal plane. The separation of 3.11(1) Å between Pt(1) and I(1) is too long to envisage a bridging position for this ligand, the same applies to I(2) (3.54(1) Å for the I(2) - Pt(3) distance). All atoms linked to the Pt_3 triangle, I(1), I(2), P(1) to P(5), lie out of the mean plane formed by the metal atoms, I(1) at +2.552(5) Å, I(2) at –1.644(5) Å, P(1) at -0.310(5) Å, P(2) at –0.214(5) Å, P(3) at 0.081(5) Å, P(4) at –1.172(5) Å and P(5) at 0.960(5) Å.

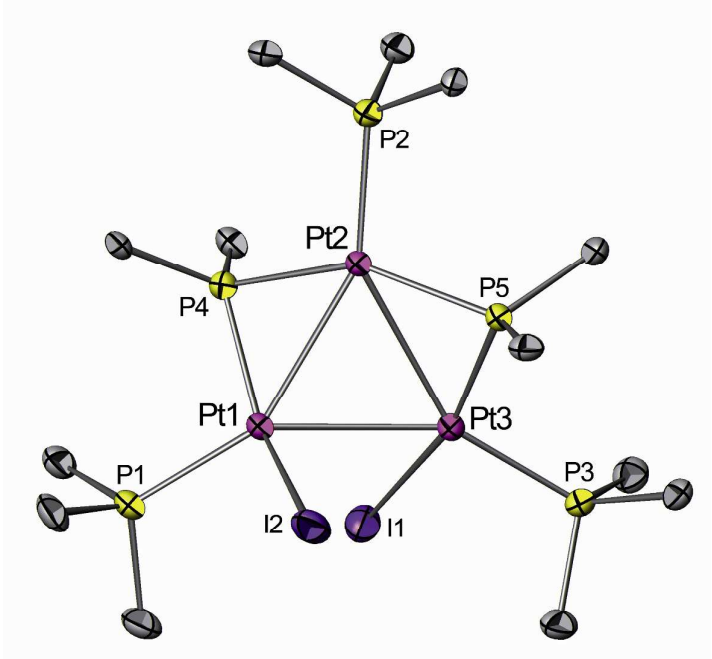

Figure 3. ORTEP view of **5** in $[Pt_3(\mu\text{-}PPh_2)_2I_2(PPh_3)_3]$·PhCl (**5**·PhCl) with partial labelling scheme. The ellipsoids enclose 50% of the electronic density. Only the ipso phenyl carbons are shown for clarity.

Table 3. Selected Bond Distances (Å) and Angles (°) in $[Pt_3(\mu\text{-}PPh_2)_2I_2(PPh_3)_3]\cdot PhCl$ (**5**·PhCl)

Pt(1) – Pt(2)	2.8330(6)	P(4)–Pt(1)–P(1)	102.77(5)
Pt(1) – Pt(3)	2.8334(6)	P(1)–Pt(1)–I(2)	95.25(4)
Pt(2) – Pt(3)	2.8835(7)	P(4) –Pt(1) –I(2)	141.54(4)
Pt(1) – P(1)	2.2674(13)	Pt(1)–Pt(2)–Pt(3)	59.42(1)
Pt(1) – P(4)	2.2143(12)	Pt(1)–Pt(2)–P(4)	49.95(3)
Pt(1) – I(2)	2.7238(7)	Pt(3)–Pt(2)– P(5)	49.26(3)
Pt(2) – P(2)	2.2603(12)	P(2)–Pt(2)–P(4)	105.69(5)
Pt(2) – P(4)	2.2700(12)	P(2)–Pt(2)–P(5)	104.41(4)
Pt(2) – P(5)	2.2669(13)	Pt(1)–Pt(3)–Pt(2)	59.40(2)
Pt(3) – P(3)	2.2511(13)	Pt(1)–Pt(3)–I(1)	67.98(1)
Pt(3) – P(5)	2.2184(12)	Pt(2)–Pt(3)–P(5)	50.74(3)
Pt(3) – I(1)	2.7278(6)	P(5)–Pt(3)–P(3)	102.60(4)
Pt(2)–Pt(1)–Pt(3)	61.18(1)	P(3)–Pt(3)–I(1)	89.78(3)
Pt(2)–Pt(1)–P(4)	51.70(3)	Pt(1)–P(4)–Pt(2)	78.35(4)
Pt(3)–Pt(1)–I(2)	80.37(2)	Pt(2)–P(5)–Pt(3)	80.00(4)

All the characterizing data for the reaction products **2-5** obtained from the trinuclear cluster **1** show that recombination of a bridging PPh_2 group with the terminal phenyl group of **1** has occurred. The initial two-electron oxidation of the cluster is thus followed by a two-electron, intramolecular reductive elimination reaction involving these ligands (Ph + PPh_2 = PPh_3). Thus, overall, the neutral 44 electron precursor cluster **1** is transformed in a cationic (**2-4**) or neutral (**5**) cluster which retains a 44 electron count.

Mixed-Metal Adducts of the Neutral Cluster $[Pt_3(\mu\text{-}PPh_2)_3Ph(PPh_3)_2]$ (1).

In the first characterized platinum–gold cluster, $[PtCl(AuPPh_3)_2(PEt_3)_2]^+$, a d^8 Pt(II) centre stabilizes a formally neutral digold unit, isolobal to H_2, to form a triangular structure characterized by two-electron, three-centre metal-metal bonding (Scheme 1).[11]

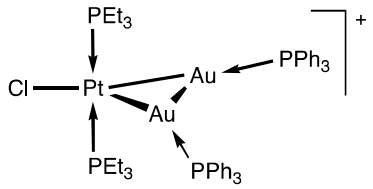

Scheme 1. Structure of the first Pt-Au cluster.[11]

It was subsequently shown that various trinuclear platinum carbonyl clusters with a 42 or 44 electron count can form addition complexes with electrophilic reagents such as $M(PPh_3)^+$ (M = Cu, Ag, Au) or HgX units.[12,13] The 44 electron cluster **1** has now been found to react with $[Cu(NCMe)_4]^+$ and $[Au(PPh_3)]^+$ to afford cationic, mixed-metal clusters $[Pt_3\{\mu_3\text{-}Cu(NCMe)_2\}(\mu\text{-}PPh_2)_3Ph(PPh_3)_2]PF_6$ (**6**(PF_6)) and $[Pt_3\{\mu_3\text{-}Au(PPh_3)\}(\mu\text{-}PPh_2)_3Ph(PPh_3)_2](TFA)$ (**7**(TFA)), which are related to the Pt_3Ag cluster $[Pt_3\{\mu_3\text{-}Ag(TFA)\}(\mu\text{-}PPh_2)_3Ph(PPh_3)_2]$ (**8**) obtained by reaction of **1** with Ag(TFA).[9] The metallic skeleton of the latter adduct has a $AgPt_3$ butterfly structure (with a long P(1)-Pt(2) separation of 3.3247(6) Å, see scheme in Table 4), the core of the precursor cluster **1** being capped by a triply bridging Ag(TFA) group.

The FAB mass-spectrum of **6**(PF_6) contains a peak corresponding to $[M\text{-}PF_6]^+ = [Pt_3\{\mu_3\text{-}Cu(NCMe)_2\}(\mu\text{-}PPh_2)_3Ph(PPh_3)_2]^+$. The presence of two molecules of acetonitrile in the complex cation of **6** is confirmed by the integration of their ^1H NMR peaks. The FAB mass-spectrum of **7**(TFA) contains the peak corresponding to $[M\text{-}TFA]^+ = [Pt_3\{\mu_3\text{-}Au(PPh_3)\}(\mu\text{-}PPh_2)_3Ph(PPh_3)_2]^+$, as well as that of $[M\text{-}TFA\text{-}Au(PPh_3)]^+$.

Table 4. Comparison of the $^{31}P\{^{1}H\}$ NMR data (δ in ppm, *J* in Hz, in THF) of the clusters $[Pt_3(\mu_3\text{-}[m])(\mu\text{-}PPh_2)_3Ph(PPh_3)_2]X_n$ (only partial data were reported before for **8**[9]).

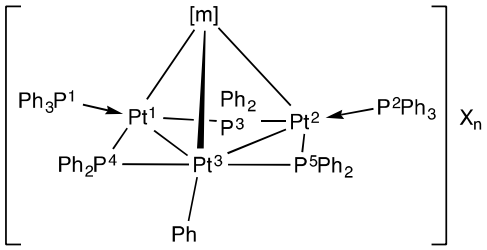

6 [m] = $Cu(NCMe)_2$; X = PF_6; n = 1
7 [m] = $Au(PPh_3)$; X = TFA; n = 1
8 [m] = Ag(TFA); n = 0

	6	**7**	**8**
$\delta_{P(1)}$ / $\delta_{P(2)}$	17.2	21.3	16.6
$\delta_{P(3)}$	-7.2	-32.9	7.6
$\delta_{P(4)}$ / $\delta_{P(5)}$	45.3	24.3	52.3
$\delta_{P(6)}$		8.2	
$^{1}J_{P(3)Pt(1)}$ / $^{1}J_{P(3)Pt(2)}$	1884	1910	1950
$^{2}J_{P(3)P(1)}$ / $^{2}J_{P(3)P(2)}$		12	13
$^{2}J_{P(3)P(4)}$ / $^{2}J_{P(3)P(5)}$	213	220	209
$^{1}J_{P(1)Pt(1)}$ / $^{1}J_{P(2)Pt(2)}$	4750	4930	4960
$^{2}J_{P(1)Pt(3)}$ / $^{2}J_{P(2)Pt(3)}$	164		183
$^{2}J_{P(1)Ag}$ / $^{2}J_{P(2)Ag}$			40 and 35
$^{3}J_{P(1)P(2)}$	75	55	90
$^{1}J_{P(4)Pt(1)}$ / $^{1}J_{P(5)Pt(2)}$	2008	2003	2050
$^{1}J_{P(4)Pt(3)}$ / $^{1}J_{P(5)Pt(3)}$	1908	1952	1990
$^{2}J_{P(4)Pt(2)}$ / $^{2}J_{P(5)Pt(1)}$	78	75	75
$^{2}J_{P(4)P(5)}$	216	230	240
$^{2}J_{P(6)Pt}$		194	
$^{3}J_{P(3)P(6)}$		11	
$^{3}J_{P(1)P(6)}$ / $^{3}J_{P(2)P(6)}$		23	

The new clusters **6** and **7** have $^{31}P\{^{1}H\}$ NMR spectra similar to that of **8**,[9] which attests the similarity of their core structures (see Table 4). In addition, the spectrum of cluster **7** contains, at 8.2 ppm, the signal of the P(6) nucleus, ligated to the Au atom, which shows couplings with the ^{195}Pt nuclei and with P(1)-P(3). These observations suggest that the structures of **6-8** are similar, i.e.

possess a tetranuclear, butterfly skeleton resulting from the capping of the precursor cluster **1** with the incoming electrophilic metal fragment.

Adducts of the Cationic Clusters $[Pt_3(\mu\text{-}X)(\mu\text{-}PPh_2)_2(PPh_3)_3]^+$ (**3**, X = OH; **4**, X = Cl)

As an extension to the reaction showing the ability of **1** to react with the electrophilic metal reagent Ag(TFA) to give $[Pt_3\{\mu_3\text{-}Ag(TFA)\}(\mu\text{-}PPh_2)_3Ph(PPh_3)_2]$,[9] it appeared interesting to examine whether the cationic, and thus less electron-rich clusters **3**(OH) and **4**(Cl) would still be able to form adducts with this or similar electrophilic reagents.

Clusters **3**(BF_4) and **4**(BF_4) reacted similarly with one equiv. of Ag(TFA) to afford the cationic clusters $[Pt_3\{\mu_3\text{-}Ag(TFA)\}(\mu\text{-}PPh_2)_2(\mu\text{-}OH)(PPh_3)_3](BF_4)$ (**9**(BF_4)) and $[Pt_3\{\mu_3\text{-}Ag(TFA)\}(\mu\text{-}PPh_2)_2(\mu\text{-}Cl)(PPh_3)_3](BF_4)$ (**10**(BF_4)), respectively. The FAB mass spectrum of **10**(BF_4) contains a peak at *m/z* = 1998.0, corresponding to the cation $[Pt_3\{\mu_3\text{-}Ag(TFA)\}(\mu\text{-}PPh_2)_2(\mu\text{-}Cl)(PPh_3)_3]^+$.

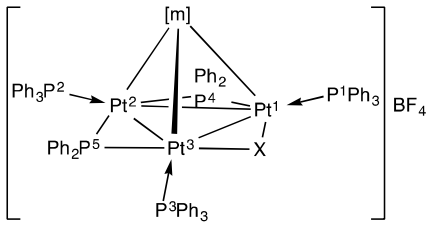

9(BF_4) [m] = Ag(TFA); X = OH
10(BF_4) [m] = Ag(TFA); X = Cl
11(BF_4) [m] = $AgBF_4$; X = I

The $^{31}P\{^1H\}$ NMR spectrum of this complex shows the signals for five phosphorus nuclei and their satellites owing to ^{31}P-^{195}Pt couplings (Table 5 and Figure 4).

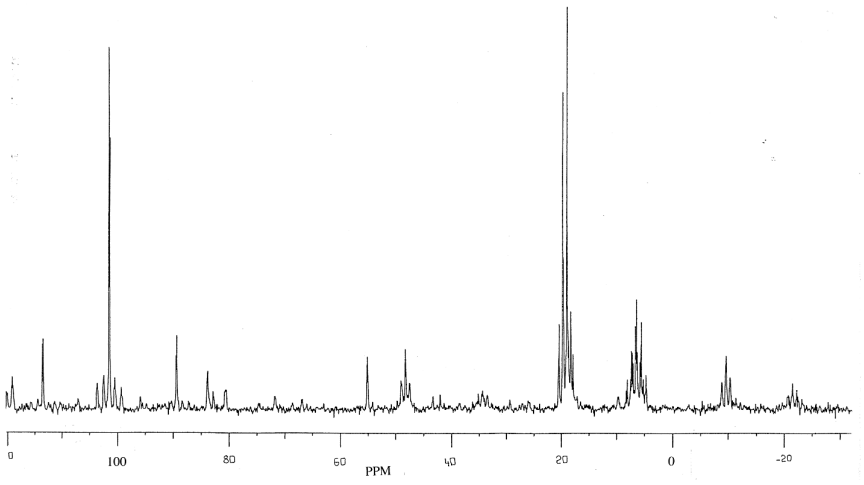

Figure 4. $^{31}P\{^1H\}$ NMR spectrum of $[Pt_3\{\mu_3\text{-}Ag(TFA)\}(\mu\text{-}PPh_2)_2(\mu\text{-}Cl)(PPh_3)_3]BF_4$ (**10**(BF_4)) in CH_2Cl_2.

The P-Ag couplings are not observed in the spectrum. The isotopomer without ^{195}Pt presents two doublets and one triplet of triplets. The doublet at δ = 101.3 corresponds to the phosphido bridges P(4) and P(5), coupled with P(2), and that at 19.3 ppm to the phosphines P(1) and P(3), which are chemically equivalent in solution and also coupled with P(2). The resonance for P(2) thus gives rise to the triplet of triplets. The couplings between chemically equivalent phosphorus nuclei, $^{2}J_{P(4)-P(5)}$ = 255 Hz and $^{3}J_{P(1)-P(3)}$ = 62 Hz, appear only in the spectra of the isotopomers containing one or two ^{195}Pt nuclei, because then the molecule becomes unsymmetrical. The signals due to the isotopomer with three ^{195}Pt nuclei, of natural abundance = 3.86%, do not appear in the experimental spectrum.

The $^{31}P\{^{1}H\}$ NMR spectrum of the cluster cation **9** (Figure S-2) is comparable to that of **10** (Table 5 and Figure 4), the only appreciable difference lying in the chemical shift of the phosphido bridges: δ(phosphido) = 53.9 in **9** and 101.3 in **10**. All these experimental data suggest that clusters **9** and **10** possess analogous molecular structures, comparable to that of compound **8.**

Table 5. $^{31}P\{^{1}H]$ NMR data (δ in ppm, *J* in Hz) of the cations $[Pt_3\{\mu_3\text{-}Ag(TFA)\}(\mu\text{-}X)(\mu\text{-}PPh_2)_2(PPh_3)_3]^+$ (**9**, X = OH; **10**, X = Cl) (TFA = $OC(O)CF_3$)

	9[a]	**10**[b]
$\delta_{P(1)}$ / $\delta_{P(3)}$	19.2	19.3
$\delta_{P(2)}$	5.0	6.4
$\delta_{P(4)}$ / $\delta_{P(5)}$	53.8	101.3
$^{2}J_{P(2)Pt(1)}$ / $^{2}J_{P(2)Pt(3)}$	154	147
$^{1}J_{P(2)Pt(2)}$	4583	4527
$^{3}J_{P(1)P(2)}$ / $^{3}J_{P(2)P(3)}$	64	62
$^{2}J_{P(2)P(4)}$ / $^{2}J_{P(2)P(5)}$	11	13
$^{1}J_{P(1)Pt(1)}$ / $^{1}J_{P(3)Pt(3)}$	4813	4687
$^{2}J_{P(1)Pt(2)}$ / $^{2}J_{P(3)Pt(2)}$	125	117
$^{1}J_{P(4)Pt(1)}$ / $^{1}J_{P(5)Pt(3)}$	2923	3110
$^{1}J_{P(4)Pt(2)}$ / $^{1}J_{P(5)Pt(2)}$	1897	1947
$^{2}J_{P(4)Pt(3)}$ / $^{2}J_{P(5)Pt(1)}$	85	93
$^{2}J_{P(4)P(5)}$	244	255

[a] in THF. [b] In CH_2Cl_2

Molecular structure of the cluster $[Pt_3\{\mu_3\text{-}AgBF_4\}(\mu\text{-}PPh_2)_2(\mu_2\text{-}I)(PPh_3)_3]BF_4$ (11(BF_4))

The reaction of complex **2**(I) with $AgBF_4$ in CH_2Cl_2 afforded the cationic cluster $[Pt_3\{\mu_3\text{-}AgBF_4\}(\mu\text{-}PPh_2)_2(\mu_2\text{-}I)(PPh_3)_3]^+$ (**11**) (eq 2), associated with the anion BF_4^- as established by X-ray diffraction (Table 6 and Figures 5 and S3).

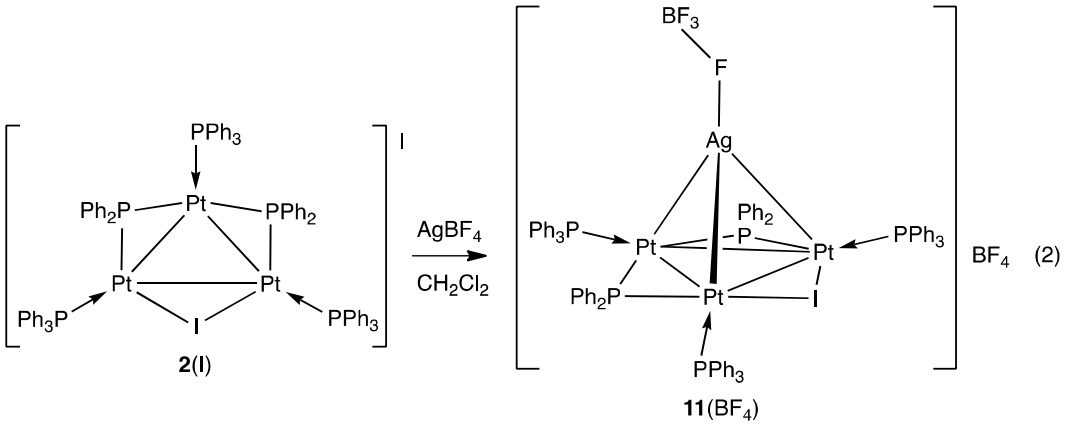

Its structure confirms that an intact $AgBF_4$ moiety has added to the Pt_3 triangle of compound **2**, with an Ag-F(1) distance of 2.35(2) Å. The structure of cation **11** is comparable to that of **8**, but with a PPh_2 bridge of **8** replaced by an iodo bridge, the phenyl group linked to a Pt atom in **8** replaced by a PPh_3 ligand in **11** and the TFA ligand in **8** replaced in **11** by a BF_4 group ligated to silver through a fluorine atom. The uncoordinated BF_4^- anion associated with cation **11** is situated under the Pt_3 plane, without direct contact with the cation. While in **8** two phosphido bridges lie above the Pt_3 plane, toward the silver cation, the other ligands being situated under the metallic plane, all the phosphorus ligands in **11**(BF_4) lean towards the Ag atom, except the bridging iodo ligand. The various Pt-P distances in **11**(BF_4) are comparable to the Pt-P distances in **1** or **4**(PF_6).[4] When comparing the core structure of **11**(BF_4) with that of the related complexes **1** and **4**(PF_6), we note that the Pt-Pt distances, comprised between 2.9344(6) and 2.9529(7) Å, are slightly shorter than in the closed structure of **1** where they range from 2.956(3) to 3.074(4) Å, but sligthly longer than in cationic **4** where they are in the range 2.825(1)-2.904(1) Å. Such metal-metal distances are known to depend from a number of parameters, including packing forces.[4] The Pt-Ag distances in the cationic cluster **11**, which range from 2.751(1) to 2.814(1) Å, are similar to those in neutral **9**, although the latter cluster has an open butterfly metallic framework. Thus, this rare addition of a neutral silver fragment to a cationic cluster results in a complex that retains the basic structure of the precursor.[14] We note that the number of structurally characterized clusters with a $AgPt_3$ core is still very limited.[12,15]

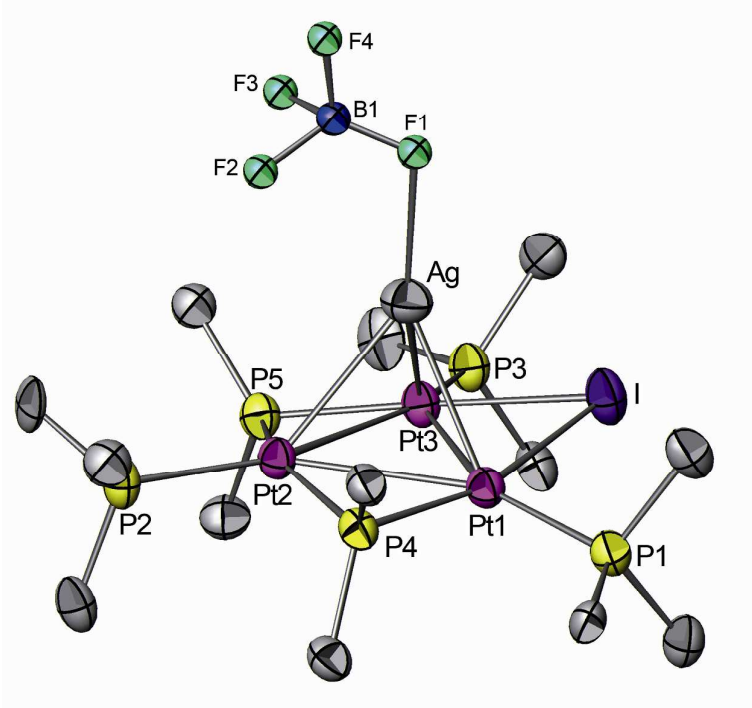

Figure 5. ORTEP view of the cationic cluster **11** in $[Pt_3(\mu_3\text{-}AgBF_4)(\mu\text{-}PPh_2)_2(\mu\text{-}I)(PPh_3)_3]BF_4$ (**11**(BF_4)) with partial labelling scheme. The ellipsoids enclose 50% of the electronic density. Only the ipso phenyl carbons are shown for clarity. Only one BF_4^- is represented for clarity.

Table 6. Selected distances (Å) and angles (°) in $[Pt_3(\mu_3\text{-}AgBF_4)(\mu\text{-}PPh_2)_2(\mu\text{-}I)(PPh_3)_3]BF_4$ (**11**(BF_4))

Pt(1) – Pt(3)	2.9529(7)	Pt(3)–Pt(1)–P(1)	145.87(8)
Pt(1) – Pt(2)	2.9344(6)	Pt(3)–Pt(1)–I	56.85(2)
Pt(2) – Pt(3)	2.9448(7)	Ag–Pt(2)–Pt(1)	58.09(2)
Pt(1) – Ag	2.795(1)	Ag–Pt(2)–Pt(3)	57.03(2)
Pt(2) – Ag	2.814(1)	Pt(3)–Pt(2)–P(2)	152.06(9)
Pt(3) – Ag	2.751(1)	Pt(3)–Pt(2)–P(5)	48.07(9)
Pt(1) – P(1)	2.253(3)	Pt(1)–Pt(2)–P(2)	147.12(9)
Pt(1) – P(4)	2.206(3)	Pt(1)–Pt(2)–P(5)	47.98(8)
Pt(2) – P(2)	2.271(3)	Pt(1)–Pt(3)–Pt(2)	59.67(2)
Pt(2) – P(4)	2.289(3)	Ag–Pt(3)–Pt(1)	58.55(2)
Pt(2) – P(5)	2.282(3)	Ag–Pt(3)–Pt(2)	59.11(3)
Pt(3) – P(3)	2.269(3)	Pt(2)–Pt(3)–P(3)	154.34(8)
Pt(3) – P(5)	2.215(3)	Pt(1)–Pt(3)–P(3)	144.00(8)
Pt(1)–I	2.678(1)	Pt(2)–Pt(3)–P(4)	50.08(8)
Pt(3) – I	2.6915(9)	Pt(1)–Pt(3)–I	56.43(2)

Ag–F(1)	2.351(17)	Pt(1)–Ag–Pt(2)	63.08(2)
Pt(2)–Pt(1)–Pt(3)	60.02(2)	Pt(1)–Ag–Pt(3)	64.33(2)
Pt(1)–Pt(2)–Pt(3)	60.30(2)	Pt(2)–Ag–Pt(3)	63.87(3)
Ag–Pt(1)–Pt(2)	58.78(2)	F(1)-Ag-Pt(1)	140.9(4)
Ag–Pt(1)–Pt(3)	57.12(3)	F(1)-Ag-Pt(2)	140.2(5)
Pt(2)–Pt(1)–P(1)	152.58(8)	F(1)-Ag-Pt(3)	145.8(5)
Pt(2)–Pt(1)–P(4)	50.48(8)	Pt(1)-P(4)-Pt(2)	81.48(11)
		Pt(2)–P(5)–Pt(3)	81.81(10)
		Pt(1)–I–Pt(3)	66.72(2)

Conclusion

In this study, we have observed that the 44 electron cluster $[Pt_3(\mu\text{-}PPh_2)_3Ph(PPh_3)_2]$ (**1**) readily reacts with protons and with electrophilic metal reagents. Protonations reactions have led to cationic clusters of type **2**-**4**, in which reductive coupling between the phenyl ligand and a phosphido bridge of the precursor has occurred to form a PPh_3 ligand. This phenomenon is similar to the oxidatively-induced reductive coupling observed when **1** was reacted with iodine.[9] It is conceivable that the first step of the cluster protonation is the formation of a species containing a bridging hydride, although we have no spectroscopic evidence for it. When the protonation reaction was carried out with an acid associated with a non-coordinating anion, such as HPF_6, in the presence of water, a cationic cluster was formed which contains a μ_2-OH ligand, which is readily displaced by a halide ligand. Upon recrystallization of the ionic cluster $[Pt_3(\mu\text{-}I)(\mu\text{-}PPh_2)_2(PPh_3)_3]I$ (**2**(I)) from chlorobenzene, its neutral formula isomer $[Pt_3(\mu\text{-}PPh_2)_2I_2(PPh_3)_3]$ (**5**) was obtained, which illustrates further the importance of the solvents. Reactions of **1** or of the cationic clusters **3** and **4** with electrophilic reagents from the group 11 metals led to mixed-metal adducts that were structurally characterized in the case of $[Pt_3\{\mu_3\text{-}Ag(TFA)\}(\mu\text{-}PPh_2)_3Ph(PPh_3)_2]$ (**8**)[9] and of $[Pt_3(\mu_3\text{-}AgBF_4)(\mu\text{-}I)(\mu\text{-}PPh_2)_2(PPh_3)_3]BF_4$ (**11**). These reactions provide chemical evidence for the fact that the cationic Pt_3 clusters investigated are still sufficiently electron-rich to react with electrophiles.

Experimental section.

All reactions were performed in Schlenk-type vessels. Solvents were dried and distilled under nitrogen. Reagents were used as received, without further purification. $[Pt_3(\mu\text{-}PPh_2)_3Ph(PPh_3)_2]$ (**1**) was prepared as reported in the literature.[4] The infrared spectra were recorded on a Bruker IFS

66 spectrophotometer and the NMR spectra on a FT-Bruker WP 200 SY instrument at 81.02 MHz ($^{31}P\{^{1}H\}$) and 200.13 MHz (^{1}H). Phosphorus chemical shifts were externally referenced to 85% H_3PO_4 in H_2O, with downfield chemical shifts reported as positive. Mass spectra were recorded on a VG ZAB-HF mass spectrometer in NBA (*m*-$O_2NC_6H_4CH_2OH$), 2NPOE (*o*-$O_2NC_6H_4OC_8H_{17}$) or magic bullet ($HSCH_2CH(OH)CH(OH)CH_2SH$) matrix. The purity of the reaction mixtures was monitored by $^{31}P\{^{1}H\}$ NMR and showed only one product obtained in quantitative yield.

[Pt$_3$(μ-I)(μ-PPh$_2$)$_2$(PPh$_3$)$_3$]I (**2**(I))

This cluster has been reported before[9] but characterization details are now provided. Solid I_2 (12.7 mg, 0.05 mmol) was added to a solution of [Pt$_3$(μ-PPh$_2$)$_3$Ph(PPh$_3$)$_2$] (**1**) (87.1 mg, 0.05 mmol) in THF (100 ml) and the mixture was stirred at room temperature for 4 h. The $^{31}P\{^{1}H\}$ NMR of the solution showed only one product, obtained in almost quantitative yield. Anal. calcd for $C_{78}H_{65}I_2P_5Pt_3$ (*M* = 1996.29): C, 46.93; H, 3.28. Found: C, 47.04; H, 3.49. FABMS (NBA matrix): *m/z* = 1869.0 ([Pt$_3$(μ-I)(μ-PPh$_2$)$_2$(PPh$_3$)$_3$]$^+$ = (*M*-I)$^+$), 1606.0 ([*M*-I-PPh$_3$]$^+$), 1148.9 ([*M*-I-Pt-2PPh$_3$]$^+$). Details of the $^{31}P\{^{1}H\}$ NMR (THF/C_6D_6) data are summarized in Table 1.

[Pt$_3$(μ-I)(μ-PPh$_2$)$_2$(PPh$_3$)$_3$]BF$_4$ (**2**(BF_4))

1) $AgBF_4$ (5.0 mg, 0.026 mmol) was added to a solution of [Pt$_3$(μ-I)(μ-PPh$_2$)$_2$(PPh$_3$)$_3$]I (50 mg, 0.025 mmol) in THF (10 ml). The mixture was stirred for 30 min. and filtered through Celite. Evaporation of the filtrate to dryness afforded an orange solid, and its purity was monitored by $^{31}P\{^{1}H\}$ NMR (THF/C_6D_6).

2) Solid I_2 (3.3 mg, 0.013 mmol) was added to a solution of [Pt$_3$(μ-OH)(μ-PPh$_2$)$_2$(PPh$_3$)$_3$](BF4) (46 mg, 0.025 mmol) in THF (10 ml). The mixture was stirred for 30 min and filtered through Celite. Evaporation of the filtrate to dryness afforded an orange solid, and its purity was monitored by $^{31}P\{^{1}H\}$ NMR (CH_2Cl_2/C_6D_6). Details of the spectra are summarized in Table 1.

[Pt$_3$(μ-OH)(μ-PPh$_2$)$_2$(PPh$_3$)$_3$]BF$_4$ (**3**(BF_4))

A mixture of **1** (174.2 mg, 0.10 mmol) and $AgBF_4$ (22.5 mg, 0.11 mmol) in THF (8 ml) was stirred at room temperature for 1 day. After filtration through Celite, addition of diethylether to the filtrate afforded yellow-orange crystals (93.8 mg, 50.8% based on Pt). Anal. calcd for

$C_{78}H_{66}BF_4OP_5Pt_3$ (*M* = 1846.39): C, 50.74; H, 3.60. Found: C, 49.42; H, 3.60. IR (KBr pellet): 1056 (s) cm^{-1} (BF_4^-). FABMS (2NPOE matrix): *m/z* = 1759.3 ($[Pt_3(\mu\text{-}OH)(\mu\text{-}PPh_2)_2(PPh_3)_3]^+$ = $M\text{-}BF_4^+$), 1742.1 ($[Pt_3(\mu\text{-}PPh_2)_2(PPh_3)_3]^+$ = $[M\text{-}BF_4\text{-}OH]^+$). Details of the $^{31}P\{^1H\}$ NMR (THF/C_6D_6) data are summarized in Table 1.

$[Pt_3(\mu\text{-}Cl)(\mu\text{-}PPh_2)_2(PPh_3)_3](BF_4)$ (**4**(BF_4))

A CH_2Cl_2 solution of **[**$Pt_3(\mu\text{-}OH)(\mu\text{-}PPh_2)_2(PPh_3)_3](BF_4)$ turned slowly yellow at room temperature. Its purity was monitored by $^{31}P\{^1H\}$ NMR and showed the presence of only one product, obtained in almost quantitative yield. Anal. calcd for $C_{78}H_{65}BClF_4P_5Pt_3$ (*M* = 1864.74): C, 50.24; H, 3.51. Found: C, 50.06; H, 3.56. IR (KBr pellet): 1056 (s) cm^{-1} (BF_4^-). FABMS (NBA matrix): *m/z* = 1777.3 ($[Pt_3(\mu\text{-}Cl)(\mu\text{-}PPh_2)_2(PPh_3)_3]^+$ = $M\text{-}BF_4^+$), 1515.2 ($[M\text{-}BF_4\text{-}PPh_3]^+$). Details of the $^{31}P\{^1H\}$ NMR (THF/C_6D_6) data are summarized in Table 1.

$[Pt_3(\mu\text{-}PPh_2)_2I_2(PPh_3)_3]$ (**5**)

When cluster **2**(I)[9] was recrystallized from chlorobenzene/hexane, all the dark red crystals formed corresponded to a neutral formula isomer **5**, as established by the structural determination of $[Pt_3(\mu\text{-}PPh_2)_2I_2(PPh_3)_3]\cdot PhCl$ (**5**·PhCl).

$[Pt_3\{\mu_3\text{-}Cu(NCMe)_2\}(\mu\text{-}PPh_2)_3Ph(PPh_3)_2]PF_6$ (**6**(PF_6))

A mixture of **1** (88 mg, 0.05 mmol) and $[Cu(NCMe)_4]PF_6$ (18.9 mg, 0.05 mmol) in THF (5 ml) was stirred at room temperature for 1 h. Addition of hexane precipitated **6**(PF_6) as a brown powder. Anal. calcd for $C_{82}H_{71}CuF_6N_2P_6Pt_3$ (*M* = 2033.10): C, 48.44; H, 3.52; N, 1.38. Found: C, 48.33; H, 3.40; N, 1.43. IR (KBr pellet): 840 (s) cm^{-1} (PF_6^-). FABMS (NBA matrix): *m/z* = 1805.1 ($[CuPt_3(\mu\text{-}PPh_2)_3Ph(PPh_3)_2]^+$ = $[M\text{-}PF_6\text{-}2MeCN]^+$), 1741.2 ($[Pt_3(\mu\text{-}PPh_2)_3Ph(PPh_3)_2]^+$ = $[M\text{-}PF_6\text{-}Cu(NCMe)_2]^+$. ^1H NMR (CD_2Cl_2): δ 7.41-6.40 (m, 65 H, aromatic H), 2.25 (s, 6 H, MeCN). Details of the $^{31}P\{^1H\}$ NMR (THF/C_6D_6) data are summarized in Table 4.

$[Pt_3\{\mu_3\text{-}Au(PPh_3)\}(\mu\text{-}PPh_2)_3Ph(PPh_3)_2]TFA$ (**7**(TFA))

A mixture of CH_2Cl_2 and MeOH (1/1, 10 ml) was added to solid [AuCl(PPh_3)] (54 mg, 0.11 mmol) and Ag(TFA) (25 mg, 0.11 mmol) and the mixture stirred for 10 min. After filtration

through Celite to remove the AgCl formed, the solvent was evaporated to dryness, the residue dissolved in THF (10 ml) and the solution added to a suspension of **1** (191 mg, 0.11 mmol) in THF (20 ml). After the reaction mixture was stirred for 2 d. at room temperature, it was concentrated under reduced pressure and addition of hexane precipitated [Pt_3{μ3-Au(PPh_3)}(μ-PPh_2)$_3$Ph(PPh_3)$_2$]TFA (**7**(TFA)). Anal. calcd for $C_{98}H_{80}AuF_3O_2P_6Pt_3$ (M = 2314.75): C, 50.85; H, 3.48. Found: C, 50.70; H, 3.75. IR (KBr pellet): 1691 (s), 1200 (s) and 1124 (s) cm^{-1} (TFA). FABMS (NBA matrix): m/z = 2200.6 ([$AuPt_3$(μ-PPh_2)$_3$Ph(PPh_3)$_3$]$^+$ = (M-TFA)$^+$, 1740.6 ([Pt_3(μ-PPh_2)$_3$Ph(PPh_3)$_2$]$^+$ = [M-TFA-Au(PPh_3)]$^+$). Details of the $^{31}P\{^1H\}$ NMR data (THF/C_6D_6) are summarized in Table 4.

[Pt_3(μ3-Ag(TFA)}(μ-PPh_2)$_3$Ph(PPh_3)$_2$] (8)

A mixture of **1** (192 mg, 0.11 mmol) and Ag(TFA) (22.8 mg, 0.10 mmol) in THF (10 ml) was stirred at room temperature for 2 d. Addition of hexane precipitated cluster **8** as a brown powder. Recrystallization from a mixture of toluene, benzene and hexane afforded brown crystals of compound **8**·C_6H_6. Anal. calcd for $C_{86}H_{71}AgF_3O_2P_5Pt_3$ (M = 2041.50): C, 50.60; H, 3.51. Found: C, 49.62; H, 3.57. IR (KBr pellet): 1669 (s), 1199 (s) and 1132 (s) cm^{-1} (CF_3CO_2). Details of the $^{31}P\{^1H\}$ NMR (THF/C_6D_6) data are summarized in Table 4.

[Pt_3{μ_3-Ag(TFA)}(μ-OH)(μ-PPh_2)$_2$(PPh_3)$_3$][BF_4] (**9**(BF_4))

Solid Ag(TFA) (13.0 mg, 0.06 mmol) was added to a solution of [Pt_3(μ-OH)(μ-PPh_2)$_2$(PPh_3)$_3$](BF_4) (**3**(BF_4)) (0.05 mmol) in THF (5 ml). This solution was stirred at room temperature for 1 h and monitoring by $^{31}P\{^1H\}$ NMR showed only the presence of [Pt_3{μ3-Ag(TFA)}(μ-OH)(μ-PPh_2)$_2$$PPh_3$)$_3$]($BF_4$) (**9**($BF_4$)) which was obtained in almost quantitative yield. Anal. calcd for $C_{80}H_{66}AgBF_7O_3P_5Pt_3$ (M = 2067.18): C, 46.48; H, 3.22. Found: C, 45.15; H, 3.20. IR (KBr pellet): 1653 (s), 1200 (s) and 1124 (s) cm^{-1} (TFA), 1062 (s) cm^{-1} (BF_4). Details of the $^{31}P\{^1H\}$ NMR (THF/C_6D_6) data are summarized in Table 5.

[Pt_3{μ_3-Ag(TFA)}(μ-Cl)(μ-PPh_2)$_2$(PPh_3)$_3$](BF_4) (**10**(BF_4))

Solid Ag(TFA) (22.1 mg, 0.10 mmol) was added to a suspension of [Pt_3(μ-Cl)(μ-PPh_2)$_2$(PPh_3)$_3$](BF_4) (186.5 mg, 0.10 mmol) in THF (15 ml) under exclusion of light. The reaction mixture was stirred at room temperature for 1 day. Monitoring of the reaction was

performed by $^{31}P\{^{1}H\}$ NMR and showed only the presence of $[Pt_3(\mu\text{-}Cl)(\mu\text{-}PPh_2)_2\{\mu_3\text{-}Ag(TFA)\}(PPh_3)_3](BF_4)$, which was obtained in almost quantitative yield. Anal. calcd for $C_{80}H_{65}AgClF_7O_2P_5Pt_3$ (M = 2085.62): C, 46.07; H, 3.14. Found: C, 46.54; H, 3.47. IR (KBr pellet): 1695 (s), 1200 (s) and 1138 (s) cm^{-1} (CF_3CO_2), 1056 (s) cm^{-1} (BF_4^-). FABMS (NBA matrix): *m/z* 1998.0 $[Pt_3\{\mu_3\text{-}Ag(TFA)\}(\mu\text{-}Cl)(\mu\text{-}PPh_2)_2(PPh_3)_3]^+ = (M\text{-}BF_4)^+$, 1777.2 ($[M\text{-}BF_4\text{-}AgTFA]^+$), 1515.1 ($[M\text{-}BF_4\text{-}AgTFA\text{-}PPh_3]^+$). Details of the $^{31}P\{^{1}H\}$ NMR (CH_2Cl_2/C_6D_6) data are summarized in Table 5.

$[Pt_3\{\mu_3\text{-}AgBF_4\}(\mu\text{-}I)(\mu\text{-}PPh_2)_2(PPh_3)_3][BF_4]$ (**11**(BF_4))

Solid I_2 (20 mg, 0.08 mmol) was added to a solution of **1** (150 mg, 0.08 mmol) in 40 ml THF. After addition of solid $AgBF_4$ (64 mg, 0.32 mmol, excess), the mixture was stirred for 3 h at room temperature, filtered and evaporated to dryness. The orange residue was recrystallised from CH_2Cl_2/diethyl ether and orange crystals of complex **11(**BF_4) formed at room temperature.

Single crystal X-ray diffraction analyses.

For $[Pt_3(\mu_2\text{-}Cl)(\mu\text{-}PPh_2)_2(PPh_3)_3]PF_6$ (**4**(PF_6)), diffraction data were collected at –100 °C using an Enraf Nonius CAD4 4F diffractometer (see Table 7). Data reduction was made by SDP package[16] with decay correction. An empirical absorption correction was applied to data with programme difabs.[17] The structure concerning platinum atoms was solved by the application of direct methods using the program SHELXS-87 and subsequent sets of Fourier and difference - Fourier syntheses revealed the whole crystal structure.[18] Hydrogen atoms were introduced as fixed contributors in structure factor calculations by their computed coordinates (C-H = 0.95 Å) and isotropic temperature factors such as B(H) = 1.3 Beqv(C) $Å^2$ but not refined. The PF_6 anion has a high thermal agitation with two positions for each fluoride atom which were refined isotropically. Full least-squares refinements were performed on |F|. A final difference map revealed no significant maxima. The scattering factor coefficients and anomalous dispersion coefficients come from references 19a and 19b, respectively.[19]

For $[Pt_3(\mu\text{-}Br)(\mu\text{-}PPh_2)_2(PPh_3)_3]OH$, the procedure was similar to that for **4**(PF_6) (Table 7). Fractionnal coordinates with standard deviations, thermal parameters ($U_{i,j}$), selected interatomic distances and bond angles and least squares planes are given in the Supplemenatry material.

Diffraction data for $[Pt_3(\mu\text{-}PPh_2)_2I_2(PPh_3)_3]\cdot PhCl$ (**5**·PhCl) and $[Pt_3(\mu_3\text{-}AgBF_4)(\mu\text{-}PPh_2)_2(\mu\text{-}I)(PPh_3)_3]BF_4$ (**11**(BF_4)) were collected on a Kappa CCD diffractometer using graphite-

monochromatized Mo-Kα radiation (λ = 0.71073 Å).[20] Crystallographic and experimental details are summarized in Table 7. The structures were solved by direct methods (SHELXS-97)[21] and refined by full-matrix least-squares procedures (based on F^2, SHELXL-97) with anisotropic thermal parameters for all the non-hydrogen atoms.[22] The hydrogen atoms were introduced into the geometrically calculated positions (SHELXL-97 procedures) and refined riding on the corresponding parent atoms. No absorption correction was made (small single crystals, Table 7).

Table 7. Summary of Crystal Data and Intensity Collection

Crystal Data	$[Pt_3(\mu_2\text{-}Cl)(\mu\text{-}PPh_2)_2(PPh_3)_3]PF_6$ (**4**(PF_6))	$[Pt_3(\mu_2\text{-}Br)(\mu\text{-}PPh_2)_2(PPh_3)_3]OH$	$[Pt_3(\mu\text{-}PPh_2)_2I_2(PPh_3)_3]\cdot PhCl$ (**5**·PhCl)	$[Pt_3(\mu_3\text{-}AgBF_4)(\mu\text{-}PPh_2)_2(\mu\text{-}I)(PPh_3)_3]BF_4$ (**11**(BF_4)).
Formula	$C_{78}H_{65}ClF_6P_6Pt_3$	$C_{78}H_{66}BrOP_5Pt_3$	$C_{84}H_{70}ClI_2P_5Pt_3$	$C_{78}H_{65}AgB_2F_8IP_5Pt_3$
Formula weight	1922.41	1838.9	2108.77	2150.81
Crystal system	Monoclinic	Monoclinic	Monoclinic	Orthorhombic
Space group	*P*2$_1$/c	*P*2$_1$/c	*P*2$_1$/c	*P*bca
Cryst. dimens. (mm)	0.1 x 0.1 x 0.13	0.1 x 0.08 x 0.11	0.10 x 0.10 x 0.10	0.12 x 0.11 x 0.10
a (Å)	15.185(1)	15.206(1)	16.602(5)	20.5440(2)
b (Å)	16.940(3)	16.924(8)	23.443(5)	25.7750(4)
c (Å)	27.518(3)	27.553(2)	19.131(5)	28.9590(4)
α (°)	90	90	90.00	90
β (°)	□□□□(□)	□□□□□□	92.974(5)	90
γ (°)	90	90	90.00	90
V (Å^3)	7067.6	7082.1	7436(3)	15334.4(4)
Z	4	4	4	8
Density (g.cm^{-3})	1.79	1.725	1.884	1.826
μ(Mo-Kα) (mm^{-1})	6.42	6.97	6.649	6.271
F(000)	3843.57	3546	4024	8028
Data collection				
Temperature (K)	293	293	173(2)	293
Radiation (graphite monochromator) (Å)	Mo-Kα1 (λ = 0.70930 Å)	Mo-Kα1 (λ = 0.70930 Å)	Mo-Kα (λ = 0.71069 Å)	Mo-Kα (λ = 0.71069 Å)
Θ min - max	1 – 28	1 – 25	2.35 - 30.00	1.41 – 27.51
Dataset [h, k, l]	±h +k +l	+h +k ±l	-23/23, 0/33, 0/26	-26/26, -33/33, -37/37
Tot., Uniq. Data, *R*(int)	14309, 14309 -	10025, 10025 -	106318, 21658 0.0289	33771, 17574 0.1142
Observed data (>2σ(*I*))	5804	6864	16367	8367
Refinement				
$N_{reflec.}$, $N_{param.}$	5804, 846	6864, 792	21658, 856	33771, 854
R2, R1, wR2 wR1, GOF	- , 0.0621, - 0.0733, -	- , 0.0499, - 0.0455, -	0.0625, 0.0390, 0.0933 0.0851, 0.846	0.0620, 0.1660, 0.1502 0.1238, 1.02
Max. and aver. shift/error	0.03, 0.01	0.038, 0.01	0.001, 0.000	0.002, 0000
Min, Max. Resd Dens. (e.Å^{-3})	-1.5, 1.5	-1.1, 1.1	-1.814, 2.615	-0.966, 1.822

Acknowledgements.

We thank the Centre National de la Recherche Scientifique and the Ministère de l'Enseignement Supérieur et de la Recherche for support. We are grateful to Johnson Matthey PLC for a generous loan of platinum salts.

1 P. E. Garrou, *Chem*. *Rev*. 1981, **81**, 229; A. J. Carty, *Adv*. *Chem*. *Ser*. **1982**, *196*, 163; P. E. Garrou, *Chem*. *Rev*. 1985, **85**, 171; E. Sappa, A. Tiripicchio and P. Braunstein, *Coord*. *Chem*. *Rev*. 1985, **65**, 219 ; P. Braunstein, *Nouv*. *J. Chim*. 1986, **10**, 365; E. Sappa, A. Tiripicchio, A. J. Carty and G. E. Toogood, *Prog*. *Inorg*. *Chem*. 1987, **35**, 437; P. Mastrorilli, *Eur. J. Inorg. Chem*. 2008, 4835; P. Mastrorilli, *Dalton Trans*. 2008, 4555; V. K. Jaina and L. Jain, *Coord. Chem. Rev*. 2010, **254**, 2848; A. Arias, J. Forniés, C. Fortuño and A. Martín, *Inorg. Chim. Acta*, 2013, **407**, 189; and references cited.

2 See e.g.: R. Bender, P. Braunstein, A. Dedieu and Y. Dusausoy, *Angew. Chem., Int. Ed. Engl.* 1989, **28**, 923; T. Blum and P. Braunstein, *Organometallics* 1989, **8**, 2497; T. Blum, P. Braunstein, A. Tiripicchio and M. Tiripicchio Camellini, *Organometallics* 1989, **8**, 2504; P. Braunstein, M. Knorr, B. Hirle, G. Reinhard and U. Schubert, *Angew. Chem., Int. Ed. Engl.* 1992, **31**, 1583; P. Braunstein, E. de Jesús, A. Tiripicchio and F. Ugozzoli, *Inorg. Chem*. 1992, **31**, 411; F. Maassarani, M. F. Davidson, I. C.M. Wehman-Ooyevaar, D. M. Grove, M. A. van Koten, W. J. J. Smeets, A. L. Spek and G. van Koten, *Inorg. Chim. Acta*, 1995, **235**, 327; A. Albinati, P. Leoni, F. Marchetti, L. Marchetti, M. Pasquali and S. Rizzato, *Eur. J. Inorg. Chem*. 2008, 4092; J. Forniés, C. Fortuño, S. Ibáñez and A. Martin, *Inorg. Chem*. 2008, **47**, 5978; I. Ara, J. Forniés, C. Fortuño, S. Ibáñez, A. Martin, P. Mastrorilli and V. Gallo, *Inorg. Chem*. 2008, **47**, 9069; M. Latronico, F. Polini, V. Gallo, P. Mastrorilli, B. Calmuschi-Cula, U. Englert, N. Re, T. Repo and M. Räisänen, *Inorg. Chem*. 2008, **47**, 9779; C. Cavazza, F. Fabrizi de Biani, T. Funaioli, P. Leoni, F. Marchetti, L. Marchetti, P. Zanello, *Inorg. Chem*. 2009, **48**, 1385; E. Alonso, J. Forniés, C. Fortuño, A. Lledos, A. Martin and A. Nova, *Inorg. Chem*. 2009, **48**, 7679; J. Forniés, C. Fortuño, S. Ibáñez, A. Martin, P. Romero, P. Mastrorilli and V. Gallo, *Inorg. Chem*. 2011, **50**, 285; M. Latronico, P. Mastrorilli, V. Gallo, M. M. Dell'Anna, F. Creati, N. Re and U. Englert, *Inorg. Chem*. 2011, **50**, 3539; J. Forniés, C. Fortuño, S. Ibáñez, A. Martin, P. Mastrorilli and V. Gallo, *Inorg. Chem*. 2011, **50**, 10798, and references cited therein.

3 R. A. Dubois and P. E. Garrou, *Organometallics*, 1986, **5**, 460; G. Lavigne in "The Chemistry of Metal Cluster Complexes", D. F. Shriver, H. D. Kaesz and R. D. Adams, Eds., VCH Weinheim, Germany, 1990, pp 201-302; P. Leoni, S. Manetti and M. Pasquali, *Inorg. Chem.*, 1995, **34**, 749; I. V. Kourkine, M. B. Chapman, D. S. Glueck, K. Eichele, R. E. Wasylishen, G. P. A. Yap, L. M. Liable-Sands and A. L. Rheingold, *Inorg. Chem.*, 1996, **35**, 1478; E. Alonso, J. Forniés, C. Fortuño, A. Martín and A. G. Orpen, *Organometallics*, 2001, **20**, 850.

4 (a) R. Bender, P. Braunstein, A. Tiripicchio and M. Tiripicchio-Camellini, *Angew. Chem., Int. Ed. Engl*. 1985, **24**, 861; (b) R. Bender, P. Braunstein, A. Dedieu, P. D. Ellis, B. Huggins, P. D. Harvey, E. Sappa and A. Tiripicchio, *Inorg. Chem.* 1996, **35**, 1223.

5 J. B. Brandon and K. R. Dixon, *Can. J. Chem*. 1981, **59**,1188 ; P. Braunstein, D. Matt, O. Bars, M. Louër, D. Grandjean, J. Fischer, A. Mitschler, *J. Organomet. Chem*. 1981, **213**, 79; A. J. Carty, C. A. Fyfe, M. Lettinga, S. Johnson and L. H. Randall, *Inorg. Chem*. 1989, **28**, 4120; S. Berger, S. Braun, H.-O. Kalinowski, *NMR-Spektroskopie von Nichtmetallen*, Thieme Verlag, Stuttgart, 1993, vol. 3.

6 See e.g.: R. E. Ginsburg, R. K. Rothrock, R. G. Finke, J. P. Collman and L. F. Dahl, *J. Am. Chem. Soc.* 1979, **101**, 6550; H. Vahrenkamp, *Adv. Organomet. Chem.* 1983, 22, 169; S. Rosenberg, G. L. Geoffroy and A. L. Rheingold, *Organometallics* 1985, **4**, 1184; D. J. Brauer, G. Hessler, P. C. Knüppel and O. Stelzer, *Inorg. Chem.* 1990, **29**, 2370.

7 (a) R. Bender, S.-E. Bouaoud, P. Braunstein, Y. Dusausoy, N. Merabet, J. Raya and D. Rouag, *J. Chem. Soc., Dalton Trans.*, 1999, 735; (b) R. Bender, P. Braunstein, S.-E. Bouaoud, N. Merabet, D. Rouag, P. Zanello and M. Fontani, *New. J. Chem.* 1999, **23**, 1045; (c) C. Archambault, R. Bender, P. Braunstein and Y. Dusausoy, *J. Chem. Soc., Dalton Trans.* 2002, 4084 ; (d) R. Bender, C. Okio, R. Welter and P. Braunstein, *Dalton Trans.* 2009, 4901; (e) C. Archambault, R. Bender, Y. Dusausoy, R. Welter and P. Braunstein, *Polyhedron* 2013, **52**, 545, and references cited.

8 N. J. Taylor, P. C. Chieh and A. J. Carty, *J. Chem. Soc., Chem. Commun.* 1975, 448.

9 C. Archambault, R. Bender, P. Braunstein, A. De Cian and J. Fischer, *J. Chem. Soc., Chem. Commun.* 1996, 2729.

10 R. Bender, P. Braunstein, J. M. Jud and Y. Dusausoy, *Inorg. Chem.* 1984, **23**, 4489.

11 P. Braunstein, H. Lehner, D. Matt, A. Tiripicchio and M. Tiripicchio-Camellini, *Angew. Chem., Int. Ed. Engl.*, 1984, **23**, 304.

12 P. Braunstein, S. Freyburger and O. Bars, *J. Organomet. Chem.* 1988, **352**, C29.

13 M. F. Hallam, D. M. P. Mingos, T. Adatia and M. McPartlin, *J. Chem. Soc. Dalton Trans.* 1988, 335; A. Stockhammer, K.-H. Dahmen, T. Gerfin, L. M. Venanzi, V. Gramlich and W. Petter, *Helv. Chim. Acta*, 1991, **74**, 989; A. Albinati, K.-H. Dahmen, F. Demartin, J. M. Forward, C. J. Longley, D. M. P. Mingos and L. M. Venanzi, *Inorg. Chem.*, 1992, **31**, 2223; A. D. Burrows and D. M. P. Mingos, *Coord. Chem. Rev.* 1996, **154**, 19, and references cited therein.

14 I. D. Salter in "Comprehensive Organometallic Chemistry II", E. W. Abel, F. G. A. Stone and G. Wilkinson (Eds.), Pergamon, 1995, Vol. 10, pp 255-322; S. Sculfort and P. Braunstein, *Chem. Soc. Rev.*, 2011, **40**, 2741.

15 A. Albinati, K.-H. Dahmen, A.Togni and L. M. Venanzi, *Angew. Chem., Int. Ed.* 1985, **24**, 766; S. Bhaduri, K. Sharma, P. G. Jones and C. F. Erdbrugger, *J. Organomet. Chem.* 1987, **326**, C46; G. Douglas, M. C. Jennings, L. Manojlovic-Muir and R. J. Puddephatt, *Inorg.Chem.* 1988, **27**, 4516; A. D. Burrows, J. G. Jeffrey, J. C. Machell and D. M. P. Mingos, *J. Organomet. Chem.* 1991, **406**, 399; L. R. Falvello, J. Forniés, C. Fortuño, F. Duran and A. Martin, *Organometallics*, 2002, **21**, 2226.

16 SDP Structure Determination Package; Enraf-Nonius: Delft, The Netherlands, 1977.

17 N. Walker and D. Stuart, *Acta Cryst.*, 1983, **A39**, 159.

18 G. M. Sheldrick, SHELXS-86: *Programs for Crystal Structure Determination; University of Göttingen: Göttingen, Germany*, 1986.

19 D. T. Cromer and J. T. Waber; *International Tables for X-ray Crystallography*, 1974, Vol. IV, The Kynoch Press, Birmingham. (a) Table 2.2b; (b) Table 2.3.1.

20 Kappa CCD Operation Manual, Nonius BV, Delft, The Netherlands, 1997.

21 G. M. Sheldrick, SHELX97, Program for the refinement of crystal structures, University of Göttingen, Germany, 1997.

22 *The Crystalbuilder Project*, R. Welter, *Acta Crystallogr., Sect. A,* 2006, **62**, s252.

Reactions of the mixed-valence cluster $[Pt_3(\mu\text{-}PPh_2)_3Ph(PPh_3)_2]$ with various electrophiles have been investigated; a cationic mixed-metal $AgPt_3$ cluster has been characterised in which the neutral $AgBF_4$ unit caps a Pt_3 cation.